

Electrokinetic separation of sulphate and lead from sludge of spent lead acid battery

S. Maruthamuthu*, T. Dhanibabu, A. Veluchamy*, S. Palanichamy, P. Subramanian, N. Palaniswamy

Central Electrochemical Research Institute, Karaikudi 630 006, India

ARTICLE INFO

Article history:

Received 7 February 2011

Received in revised form 12 July 2011

Accepted 12 July 2011

Available online 22 July 2011

Keywords:

Electrokinetics

Used lead acid battery

Recovery

Lead

Sulphates

Pollutants

ABSTRACT

A novel electrokinetic (EK) technique is applied to separate lead and sulphate from the sludge of used/spent lead acid battery. XRD reveals that the sludge is a mixture of $(\text{PbO})_4$ [$\text{Pb}(\text{SO}_4)$], Pb_2O_3 , PbSO_4 , $\text{Pb}(\text{S}_2\text{O}_3)$ and $\text{Pb}_2(\text{SO}_4)$ which upon DC voltage application in a EK cell employing either titanium electrodes or titanium substrate insoluble anode as electrodes caused migration of sulphates and lead ions respectively into anode and cathode compartments, and accumulation of insoluble lead oxides at the central compartment. The insoluble lead oxides accumulated at the central compartment in the ratio 1:3, respectively for the high oxygen over-voltage Ti-anode (Ti-EK cell) and low oxygen over-voltage TSIA-anode (TSIA-EK cell) shows the superiority of Ti anode over TSIA anode. Also thermal investigation reveals Pb deposited at Ti-cathode is superior to that from TSIA cathode. This process does not release air/soil pollutants which are usually associated with high temperature pyrotechnic process.

© 2011 Elsevier B.V. All rights reserved.

1. Introduction

Since 1859, following the invention of lead acid battery by Gaston Planté, battery power requirement for the automotive and domestic applications witnessed phenomenal growth and the demand for Pb increased to the tune of several thousand tons. About 30% from Pb ore mining and 70% from recycling of used lead acid battery (ULAB) have become the source of Pb for battery manufacturing industry. The most prevalent and popular technology over several decades for the recovery of Pb from ULAB is based on pyrometallurgical route due to its process/unit operation simplicity and cost effectiveness. As this process is associated with emission of pollutants such as sulphur dioxide and fine lead particulates into air/soil environment [1–6], alternative pollution free processes based on chemical and electrochemical methods have been attempted with the result the Ginatta process, still more advanced one which eliminated air/soil pollution was developed. This process was established in the form of pilot plants by Maja et al. and others [7–12] and it involves treatment of the sludge with chemicals such as ammonium carbonate, sodium carbonate, or sodium hydroxide solutions for the removal of sulphate in the form of soluble sulphates and precipitation of Pb^{2+} ions either as PbCO_3 or $\text{Pb}(\text{OH})_2$. The precipitate is filtered and dissolved in fluo-

boric acid to obtain an electrolyte containing Pb^{2+} ions which upon subjecting to electrowinning process, Pb was recovered at the cathode. Further, later on this process underwent a modification in the cell design by incorporating a diaphragm which eliminated problems such as dendritic deposition at the cathode and parasitic PbO_2 formation over the anode. Acidic electrolyte (HBF_4) containing Pb^{2+} ions and Fe/Fe^{2+} couple separated by a membrane selective to Pb^{2+} ions have been designed. In this cell Pb^{2+} was reduced at the cathode with a simultaneous oxidation of Fe particles at the anode [8,12].

Maja et al. [7] suggested that during leaching process the Pb particles present in the sludge reduces higher lead oxides (PbO_x where $x > 1$) into lower oxide (PbO) which undergoes easy conversion into PbCO_3 or $\text{Pb}(\text{OH})_2$ during leaching process. Presence of 13% metal particles (Pb and Sb) in most of the sludges favored spontaneous conversion of higher valent Pb compounds into lower valent Pb compounds during leaching process. In the Brazilian ULAB by virtue of its lesser Pb metal particles ~5% posed severe problems during Pb recovery process. Followed by this process, attempts were made to develop process based on electrowinning for the recovery of Pb in alkaline solutions [13–15]. Ferracin et al. [16], carried out sulphate removal in the sludge of Brazilian by treating with NaOH, which converted all sulphates of Pb into $\text{Pb}(\text{OH})_2$. After desulphation, the sludge leached in tetrafluoroboric acid (HBF_4) was electrolyzed through electrowinning technique and deposited Pb at a current density of 250 A m^{-2} .

Volpe et al. [17] described a hydrometallurgical route in which the Pb^{2+} species in the sludge was brought into solution by the

* Corresponding authors.

E-mail addresses: biocorrcecri@gmail.com (S. Maruthamuthu), Veluchamy.a@gmail.com (A. Veluchamy).

excess acetate ions which got reduced into Pb^0 in conjunction with oxidation of Fe^0 to Fe^{3+} through the formation of Fe^{2+} reducing Pb^{4+} in PbO_2 into Pb^{2+} in the acetate solution. Fe^{3+} subsequently reacts with Fe^0 to give Fe^{2+} species. The operative condition was well set to avoid any precipitation due to low solubility of Fe (III) species.

Sonmez and Kumar [18,19] explored three independent leaching processes by treating (1) PbO with citric acid, (2) PbO_2 with citric acid in the presence of H_2O_2 and (3) PbSO_4 with sodium citrate and citric acid mixture to get lead citrate precursor for the recovery of Pb by electrowinning technique.

Authors in this paper report for the first time an Electrokinetic process for the separation of SO_4 and Pb from the sludge of ULAB. The SO_4^{2-} ions migrate towards anolyte compartment and Pb^{2+} ions into cathode compartment in an electrokinetic cell. So far this electrokinetic cell has been applied to remove Pb^{2+} ions in soil wastes [20–22].

Two different electrokinetic cells with different electrodes have been employed, one with titanium electrodes (Ti-EK cell) and the other with titanium substrate insoluble anodes as electrodes (TSIA-EK cell). XRD, Atomic absorption spectroscopy (AAS), gravimetric and thermal analyses were employed to analyze the materials involved with this EK technique to understand the mechanism underlying Pb and sulphate separation.

2. Materials and method

2.1. Electrokinetic cell

Fig. 1 shows the schematic diagram of the electrokinetic cell. The cell was constructed using acrylic sheets of dimensions $l=24$ cm; $b=4$ cm; $h=6$ cm which was divided into three compartments separated by perforated acrylic sheets. Adjacent to the acrylic sheets, filter paper was placed in order to avoid movement of sludge particles from the central compartment into anodic or cathodic compartments. The central compartment was filled with sludge mass wetted well with 0.1 M acetic acid. The anode compartment contained 0.3 M acetic acid (anolyte) and the cathode compartment with 0.01 M potassium nitrate acidified with 0.3 M acetic acid (catholyte). Two cells, one (Ti-EK cells) with titanium (Ti) electrodes and another (TSIA-EK cell) with titanium substrate insoluble anode (TSIA) as anode/cathode were subjected to EK process by applying voltage between the electrodes, and evaluated the performance of both Ti and TSIA electrodes towards Pb deposition at the cathode compartment and SO_4 accumulation at anolyte compartment. The

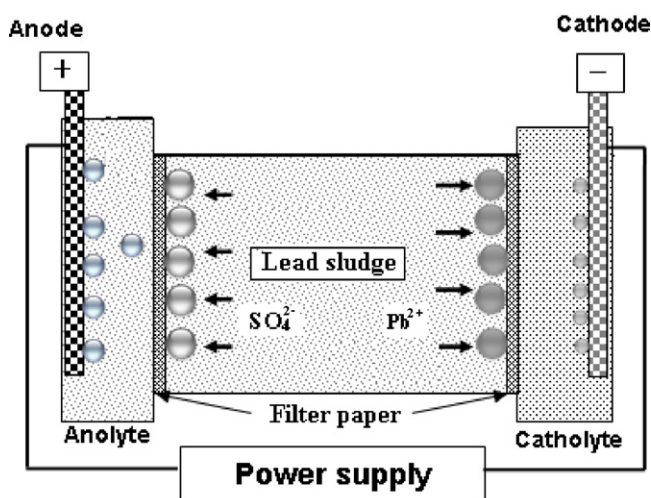


Fig. 1. The schematic diagram of electrokinetic cell.

area of the electrode, 10 cm^2 was kept constant for both electrodes. The potentials (V) referred to in this presentation were monitored with respect to normal calomel electrode potential. During the experiment, acetic acid was added to adjust the pH to ~ 5 in the cathode chamber which stabilized Pb^{2+} ions in the catholyte so as to get easy reduction at the cathode. To begin with, D.C. voltage was first applied to the EK cell by means of DC power source. The optimum voltage to obtain better separation of Pb^{2+} and SO_4^{2-} was arrived by monitoring lead deposition at the cathode and sulphate separation at the anode. This was done by varying the applied voltage to the EK cells and noted the voltages, 3 Vcm^{-1} for Ti-EK cell and 1 Vcm^{-1} for TSIA-EK are more appropriate for the operation of the EK cell.

The diagram shown in Fig. 1 depicts that during electrolysis Pb^{2+} moves to cathode and sulphate ions to the anode. Distance from the perforated acrylic sheets towards central compartment near the anode side will be referred hereinafter as normalized distance from the anode for easy understanding. Samples in the central compartment at different normalized distances from the anode side were collected periodically and analyzed for lead and sulphate contents using Atomic absorption spectroscopy (AAS) and gravimetric method respectively.

2.2. Instrumentation

The DC power required for the EK cell was provided by Aplab power supply model: Regulated DC power supply L 3205 with a variable voltage from 0 to 32 V and current from 0 to 5 A. The sulphates in the bulk before and after EK was measured by precipitating the Pb^{2+} ions as PbSO_4 and estimated gravimetrically. The pH of different compartment was noted using the pH meter: Eu Tech, pH 510 model.

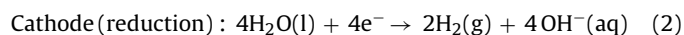
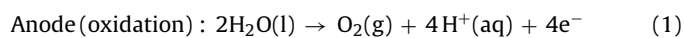
Thermal data was obtained for 'Pb' sample ($\sim 3\text{--}5$ g) placed in an alumina sample holder, kept in the chamber and subjected to a heat rate of $20^\circ\text{C}/\text{min}$ in a nitrogen atmosphere in the TGA-Q600, TA Instrument, USA provided with a data processing program universal analyzer.

The XRD pattern of the sludge before and after EK experiments was recorded using computer controlled XRD system, JEOL, and Model: JPX 8030 with $\text{CuK}\alpha$ radiation (Ni filtered = 13418 \AA) in the range, 40 kV, 20 A. The peak search and peak match program built with software (syn master 7935) was used to identify the peak table and ultimately for the identification of the compounds with the aid of JCPDS files.

Atomic absorption spectrum (VARIAN SPECTRAA 220 Model) was employed to analyze Pb contents of the sample collected at different location in the central compartment of the EK cells before and after experiments. Each sample ~ 10 mg was completely dissolved in a solution mixture made of 3% supra HNO_3 and 1% HCl and appropriately diluted to bring the lead concentration within 50 ppm and analyzed using AAS. This technique helps to find out quantitatively the amount of Pb content in the sample.

3. Results and discussion

Fig. 2 illustrates the curves representing the variation of pH with number of days for the Ti-EK and TSIA-EK cells. During the initial period of the experiment, the anolyte pH (pH 2–3) of Ti-EK cell changes into more acidic (pH 2–1) due to release of H^+ ions from the anode [22] which is represented by the reaction (1).



The 4e^- released from the anode (reaction (1)) reduces four H_2O molecules at the cathode (reaction (2)) leading to the formation of

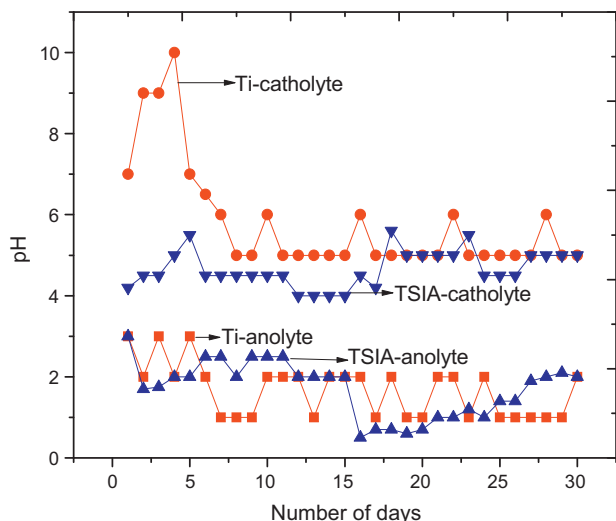


Fig. 2. Variation of pH with number of days for Ti and TSIA-EK Cells.

hydroxyl ions which increases the pH to 10 from 7 at the cathode. However, the increase of alkaline pH is periodically brought down to ~5–6 by adding appropriate quantity of acetic acid in order to stabilize Pb^{2+} to favor deposition of Pb at the cathode. The pH variation with number of days for TSIA-EK cell shows a trend which is similar to Ti-EK cell but with a slight difference in its pH variation pattern from the beginning to end of the experiment.

Fig. 3 depicts the curves which represent variation of potential (V) versus number of days for the Ti-EK and TSIA-EK cell experiments. For the Ti-EK cell, the potential of the anode remains initially at 5 V, and then slowly increases to 24 V and the potential of the cathode varies between -5 V and -0.5 V. This high cathodic potential favors reduction of Pb^{2+} ions at the cathode. Also the Ti-anode causes release of negligible oxygen in the cell by virtue of its high oxygen over voltage creating low oxidizing environment which is conducive only to the formation of low lead oxide formation. This is evident from the accumulation of low Pb oxide content in the central compartment of the Ti-EK system. Whereas in the TSIA-EK cell, the anode potential varied narrowly from 2.5 to 3.75 V and the cathode potential between -2.5 and -0.5 V. As TSIA anode has low oxygen over-voltage, is expected to effect high oxygen evolution from the anode which could favor high Pb oxide formation or

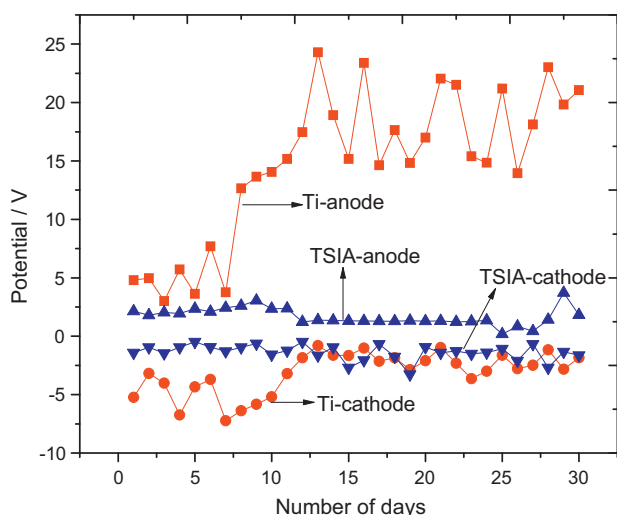


Fig. 3. Variation of potential 'V' with number of days for Ti and TSIA-EK cells.

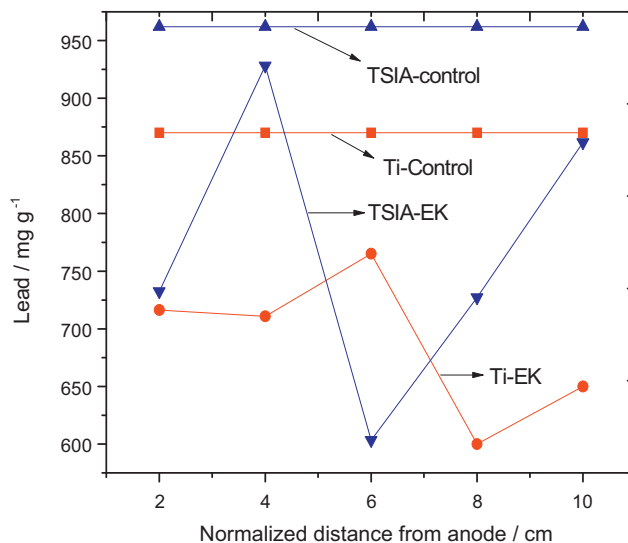


Fig. 4. Lead concentration in the bulk from normalized anode distance.

stabilize already existing lead oxides. The low cathodic potential achieved by TSIA cathode favors poor Pb^{2+} reduction. In practice, the results from TSIA cell system showed high Pb oxides near the anode side of the central compartment and low Pb deposition at the cathode.

Fig. 4 presents variation of Pb concentration in the bulk from normalized distance from Ti and TSIA anodes in the Ti-EK and TSIA-EK cells respectively. TSIA-control system, while not subjected to applied potential shows Pb content ~ 970 $mg\ g^{-1}$ at the central compartment independent of distance from the anode. It is evident from the figure that the application of voltage to the cell for 30 days caused only inconsistent values ranging from ~ 925 to 600 $mg\ g^{-1}$ with duration of experiment. The reason for the inconsistent values may be due to agitation/turbulence caused by copious oxygen released from the anode. Similarly, the Ti-control system showed Pb ~ 875 $mg\ g^{-1}$ at the central compartment independent of distance from the anode whereas the same system showed Pb content between 760 and 600 $mg\ g^{-1}$ after 30 days of EK application. Comparison of lead content values from the results suggest that Ti-EK contains less Pb content compared to TSIA-EK system in the central compartment implying more amounts of Pb ions moved out and got deposited in the cathode of Ti-EK system. But in TSIA-EK system more Pb oxides is present at the central compartment, attributed to oxidation of Pb compounds/ions into Pb oxides or lower Pb oxides into higher Pb oxides by the diffused oxygen from the low oxygen over-potential TSIA anode, which is evident from 'b' of XRD in Fig. 6. The lead oxides at the end of 30 days in the central compartment for Ti-EK and TSIA-EK cells are in the ratio 1: 3 which appears to be in proportion with the low and high oxygen evolution at Ti and TSIA anodes, dictated possibly by the oxygen-over voltages of the anodes. This shows higher oxygen over-voltage anode (Ti) favors higher Pb recovery and smaller oxide formation in the central compartment. Similarly, lower oxygen over-voltage anode (TSIA) favors lower Pb recovery and copious Pb oxide formation.

Fig. 5 shows the sulphate concentration in the central compartment from the anode side (normalized distance from the anode) of EK cell and also in the control systems of Ti and TSIA cells. The control systems are reference systems which are kept for comparing the values with EK run systems. The difference in sulphate concentration values ~ 177 and 152.41 $mg\ g^{-1}$, respectively of the Ti and TSIA control cells (Fig. 5) is due to sampling from different spent batteries. This also shows the possibility of presence of different amount of sulphates at different spent batteries in the sludges. Even

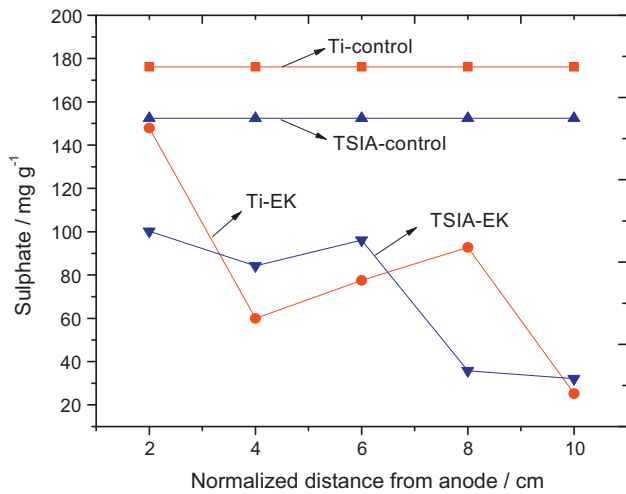


Fig. 5. The sulphate concentration in the bulk from normalized anode distance.

though Ti-control cell has higher sulphate content $\sim 177 \text{ mg g}^{-1}$ compared to 152.41 mg g^{-1} for TSIA control cell, the system at a distance of 10 cm from the anode of the EK cells after application of voltage after 30 days showed sulphate content $< 30 \text{ mg g}^{-1}$, a value which is lower compared to $\sim 35 \text{ mg g}^{-1}$ as shown in TSIA-EK cell. These results suggest the application of voltage causes migration of more sulphate ions from the central compartment to the anode side in the Ti-EK cell than that in TSIA-EK cell.

Fig. 6 depicts XRD patterns of the sludge of ULAB. The XRD 'a' for the control system shows presence of constituents such as $(\text{PbO})_4$ [$\text{Pb}(\text{SO}_4)$], Pb_2O_3 , PbSO_4 , $\text{Pb}(\text{S}_2\text{O}_3)$ and $\text{Pb}_2(\text{SO}_4)$. The XRD pattern 'b' and 'c' are obtained for the sludge material collected from the mid point of the central compartment after performing EK for 30 days. XRD pattern as in 'b' of TSIA-EK shows presence of peaks corresponding to different oxides such as Pb_3O_4 , Pb_2O_3 , $\beta\text{-Pb}_2\text{O}_3$, Pb_3O_4 , and PbO , but the XRD pattern in 'c' of Ti-EK cell shows only three peaks corresponding to the compounds such as Pb_2O_3 , PbO and Pb_3O_4 . Both 'b' and 'c' do not exhibit any peaks corresponding to sulphate indicating all sulphate ions have migrated towards anolyte/central compartment regions. For the compounds shown by the XRD (a, b, and c) diagrams, the JCPDS file numbers and other related data are given in Tables 1, 2 and 3, respectively.

The mechanism which leads to the formation/presence of oxide products in the central compartment, accumulation of sulphates

Table 1

JCPDS file numbers and other related data for the compounds shown in XRD-'a' for the sludge control system/before EK experiment. The compounds are marked as $\text{Pb}_2\text{O}_3 \rightarrow \text{O}$; $\text{PbSO}_4 \rightarrow \bullet$; $\text{Pb}(\text{S}_2\text{O}_3) \rightarrow \blacklozenge$; $(\text{PbO})_4(\text{Pb}(\text{SO}_4)) \rightarrow \blacksquare$; $\alpha\text{-Pb}_3\text{O}_2(\text{SO}_4) \rightarrow \boxtimes$; $\text{SO}_3 \rightarrow \blacklozenge$.

D spacing	Matching	Symbols	Compounds	JCPDS file number
4.18273	4.1837	\blacksquare	$(\text{PbO})_4\text{Pb}(\text{SO}_4)$	89-7618
3.66066	3.6642	\boxtimes	$\alpha\text{-Pb}_3\text{O}_2(\text{SO}_4)$	83-1767
3.46933	3.4870	\bullet	PbSO_4	89-3750
3.29739	3.2279	\bullet	PbSO_4	89-3750
2.98334	2.9848	\boxtimes	$\alpha\text{-Pb}_3\text{O}_2(\text{SO}_4)$	83-1767
2.76745	2.7633	\bullet	PbSO_4	89-7356
2.15161	2.1543	O	Pb_2O_3	89-7387
2.05414	2.0532	\blacklozenge	$\text{Pb}(\text{S}_2\text{O}_3)$	80-1698
2.01715	2.0111	\blacklozenge	SO_3	73-2169
1.96087	1.9654	\blacksquare	$(\text{PbO})_4\text{Pb}(\text{SO}_4)$	89-7618
1.74437	1.7417	\bullet	PbSO_4	89-7356
1.68736	1.6851	\blacksquare	$(\text{PbO})_4(\text{Pb}(\text{SO}_4))$	89-7618
1.61696	1.6134	\blacksquare	$(\text{PbO})_4(\text{Pb}(\text{SO}_4))$	89-7618
1.56169	1.5660	\blacklozenge	$\text{Pb}(\text{S}_2\text{O}_3)$	80-1698
1.47803	1.4793	O	Pb_2O_3	89-7387
1.26980	1.2695	\bullet	PbSO_4	89-7356

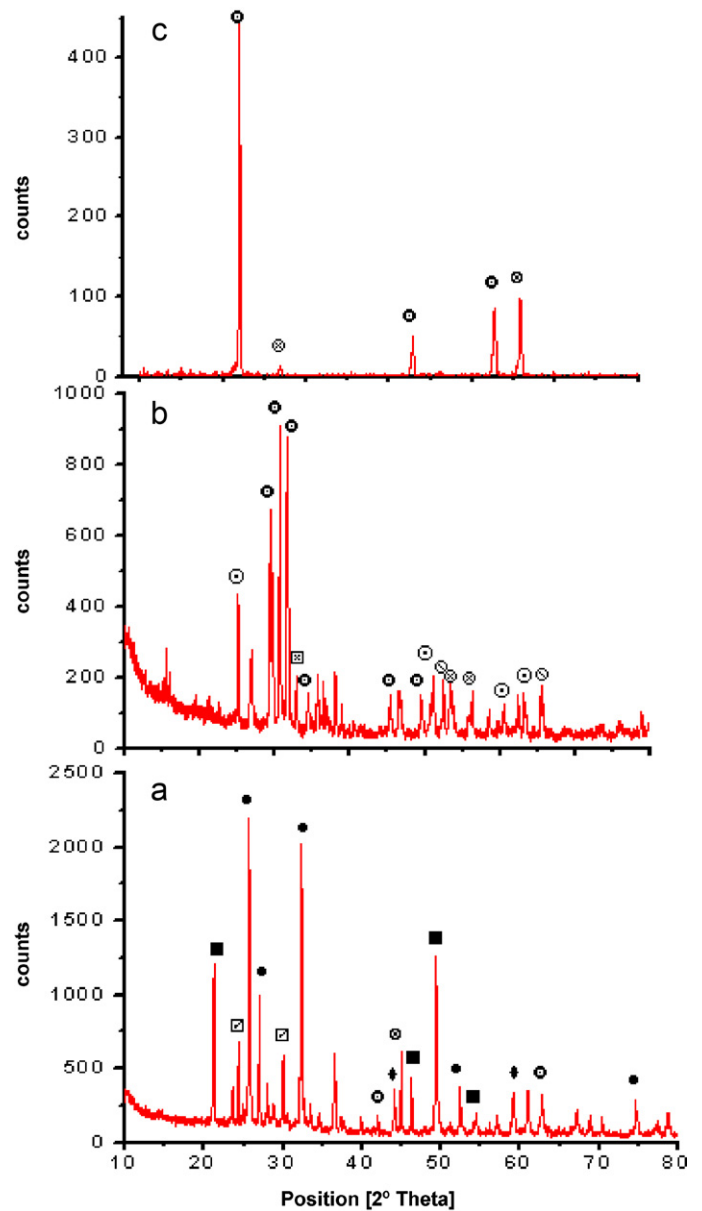


Fig. 6. X-ray diffraction spectrums: 'a' for the Sludge removed from ULAB; Sludge collected from the mid point of central compartment after 30 days of EK experiment: 'b' for TSIA-EK cell; 'c' for Ti-EK cell.

Table 2

JCPDS file numbers and other related data for the compounds shown in XRD-'b' diagram for the central compartment materials from the TSIA-EK cell. The compounds are marked as $\text{Pb}_2\text{O}_3 \rightarrow \text{O}$; $\text{PbO} \rightarrow \otimes$; $\text{Pb}_3\text{O}_4 \rightarrow \odot$; $\text{Pb} \rightarrow \ominus$; $\beta\text{-Pb}_2\text{O}_3 \rightarrow \boxtimes$.

D spacing	Matching	Symbols	Compounds	JCPDS file number
3.355757	3.5571	\odot	Pb_3O_4	65-6532
3.03337	3.0338	O	Pb_2O_3	76-1791
2.91555	2.9529	O	Pb_2O_3	76-1791
2.82772	2.8080	O	Pb_2O_3	76-1791
2.27264	2.7255	\boxtimes	$\beta\text{-Pb}_2\text{O}_3$	76-1832
2.60395	2.6031	O	Pb_2O_3	76-1791
1.99961	1.9937	O	Pb_2O_3	89-7387
1.83869	1.8320	O	Pb_2O_3	23-0331
1.79199	1.7907	\odot	Pb_3O_4	89-1947
1.74610	1.7430	\ominus	Pb	87-0663
1.71316	1.7192	\otimes	PbO	88-1589
1.63789	1.6370	\otimes	PbO	76-1796
1.52836	1.5289	\odot	Pb_3O_4	89-1947
1.46744	1.4640	\odot	Pb_3O_4	89-1947
1.42198	1.4231	\ominus	Pb	87-0663

Table 3

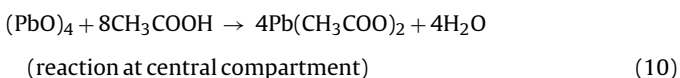
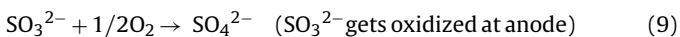
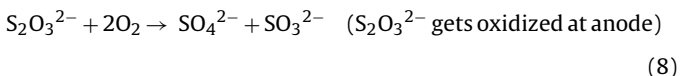
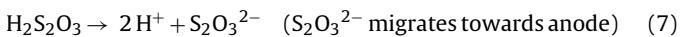
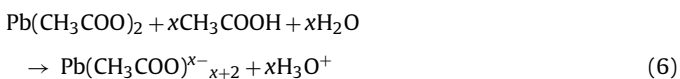
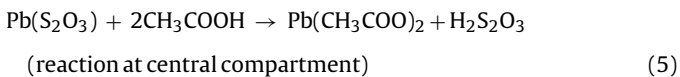
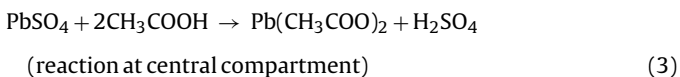
JCPDS file numbers and other related data for the compounds shown in 'c' of XRD diagram for the center compartment from the Ti-EK cell. The compounds are marked as $\text{Pb}_2\text{O}_3 \rightarrow \text{⓪}$; $\text{PbO} \rightarrow \text{ⓧ}$; $\text{Pb}_3\text{O}_4 \rightarrow \text{Ⓞ}$.

D spacing	Matching	Symbols	Compounds	JCPDS file number
2.80570	2.8080	⓪	Pb_2O_3	79-1791
2.43363	2.4337	ⓧ	PbO	65-2826
1.73213	1.7357	⓪	Pb_2O_3	79-1791
1.48101	1.4810	⓪	Pb_2O_3	76-1791
1.41726	1.4137	Ⓞ	Pb_3O_4	65-2851

in the anolyte and appearance of Pb metal in the cathode may be understood in the following passage [17,23,24].

Let us consider in the following section to explain how the materials (PbO)₄ [$\text{Pb}(\text{SO}_4)$], Pb_2O_3 , PbSO_4 , $\text{Pb}(\text{S}_2\text{O}_3)$ and $\text{Pb}_2(\text{SO}_4)$ in the central compartment leads to, (1) formation of only Pb_2O_3 species in the central compartment after 30 days of Ti-EK cell, (2) formation of large amount of different oxides near the anode side of the central compartment of TSIA-EK cell, (3) separation of lead as lead metal deposits at the cathode, and (4) accumulation of sulphates in the anolyte compartment.

We propose the possible reactions in the form of equations from 3 to 11 which explain different processes in the EK cells.



The positive ionic species H_3O^+ and Pb^{2+} migrate to the cathode where H_3O^+ is neutralized by OH^- liberated at the cathode and Pb^{2+} deposits over the cathode. The anionic species SO_4^{2-} , $\text{S}_2\text{O}_3^{2-}$ and $\text{Pb}(\text{CH}_3\text{COO})_{x-2}^{x-2}$ move towards anode. The species such as SO_4^{2-} , $\text{S}_2\text{O}_3^{2-}$ diffuses into anode compartment, $\text{S}_2\text{O}_3^{2-}$ oxidizes as SO_4^{2-} and accumulates in the anode compartment whereas the bulky ionic species $\text{Pb}(\text{CH}_3\text{COO})_{x-2}^{x-2}$ ions get hindered by the filter paper separator, encounter H^+ from the Ti-anode and splits into CH_3COOH and Pb^{2+} . Pb^{2+} migrates to cathode and undergoes deposition. In the case of TSIA-anode, the $\text{Pb}(\text{CH}_3\text{COO})_{x-2}^{x-2}$ ions

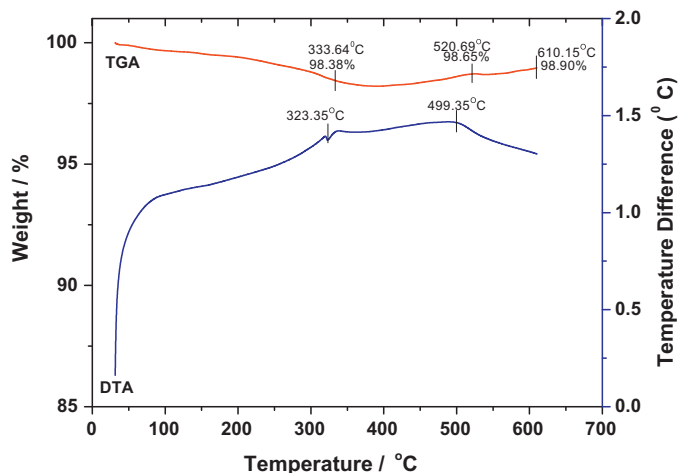


Fig. 7. Thermogravimetric analysis (TGA) and differential thermal analysis of lead collected from Ti-cathode.

hindered by the filter paper separator, encounter oxygen rich environment and get converted as various oxides (Table 2) near the anode side of the center compartment. The high intensity XRD peaks observed for Pb_2O_3 as in 'b' and 'c' suggest accumulation of large amounts of this species in the central compartment of both Ti-EK cell and TSIA-EK cells. Further, it may be noted that the intensity of all the oxide species in 'c' is much lower compared to the species present either 'a' or 'b'.

Figs. 7 and 8 represent respectively the thermogravimetric analysis (TGA) and differential thermal analysis (DTA) of the Pb collected from Ti and TSIA-EK cells. Fig. 9 shows the picture of the Pb particles deposited/collected in the cathode compartments. In Fig. 7 the inflection point in the DTA curve at 323.65°C is associated with melting point of Pb. The TGA shows that the weight loss starts before the melting point and ends after the melting point and then shows a slight increase in weight. The loss in weight suggests oxidation of any dissolved organic materials, and increase in weight suggests formation of Pb compounds by reacting with air surrounding the Pb particles. The purity of the Pb obtained is about 98.5%. In Fig. 8, the thermogravimetric analysis (TGA) graph shows weight loss upto 400°C possibly associated with evaporation of organic impurities present in the sample. The slight increase in weight above 400°C may be due to the reaction of water or other

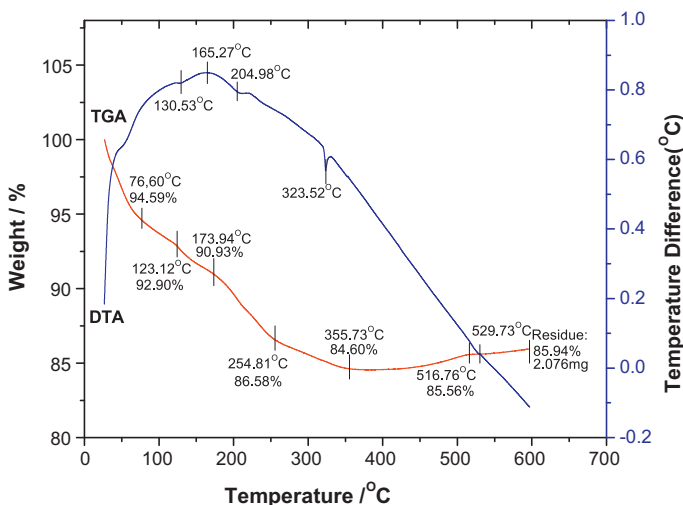


Fig. 8. Thermogravimetric analysis (TGA) and differential thermal analysis of lead collected from TSIA-cathode.



Fig. 9. Lead particles collected in the cathode compartment.

oxide impurities available in the reaction chamber that are released from the sample material. The purity of the metal is not greater than 85%. The inflection point at 323.52 in the DTA curve is due to the melting of the lead. Comparison of the thermal data available in Figs. 7 and 8 shows that the lead removed from the Ti-cathode is more superior to that recovered from TSIA-cathode.

4. Conclusion

The work presented here is to separate lead (Pb) and $\text{SO}_4/\text{S}_2\text{O}_3$ from the sludge of used lead acid battery (ULAB). This sludge, made up of $(\text{PbO})_4$ [$\text{Pb}(\text{SO}_4)$], Pb_2O_3 , PbSO_4 , $\text{Pb}(\text{S}_2\text{O}_3)$, and $\text{Pb}_2(\text{SO}_4)$ as evident from XRD results, was subjected to EK process in two different EK cells, one with Titanium (Ti) electrodes (Ti-EK cell) and another with Titanium Substrate Insoluble Anode (TSIA) electrodes (TISA-EK cell).

The Ti anode in a Ti-EK cell by virtue of its high oxygen over-voltage caused low oxygen evolution and ultimately low yield of insoluble lead oxides in the central compartment which led to better separation of sulphates and lead. On the other hand the TSIA anode with low-oxygen over-voltage liberated more oxygen which resulted in the saturation of the anode side of the cell with more amounts of oxygen at the anode which led to the formation/accumulation of large amount of oxides in the anode side and poor Pb deposits at the cathode of the TSIA-EK cell. The above results are supported further by the observation that the intensity of all the oxide species in 'c' is much lower compared to the species present in either 'a' or 'b'.

The simplicity of the experiment along with its ambient temperature operation demonstrated the EK process with Ti electrodes performs better compared to TSIA electrodes for the separation of Pb and sulphates from the sludge of ULAB. The aim of this attempt is to replace the widely employed high temperature pyrotechnique process which emits air/soil pollutants, SO_2 , and Pb and Pb oxide dust into atmosphere and also the recently developed cumbersome Ginatta process by Maja et al. [7].

Further work is in progress to improve the separation of Pb and sulphates efficiently from the sludge and also to eliminate com-

pletely the presence of lead oxides in the central compartment, finally to develop a technology which could be economically and environmentally viable one.

References

- [1] M. Stevenson, Encyclopedia of Electrochemical Power sources, 2009, 65–178.
- [2] J.L. Bourson, Recycling of lead/acid batteries in a small plant, J. Power Sources 57 (1995) 1–83.
- [3] U. Hoffmann, B. Wilson, Requirements for, and benefits of, environmentally sound and economically viable management of battery recycling in the Philippines in the wake of Basel Convention trade restrictions, J. Power Sources 8 (2000) 115–123.
- [4] A.M. Bernardes, D.C.R. Espinosa, J.A.S. Tenório, Recycling of batteries: a review of current processes and technologies, J. Power Sources 130 (2004) 291–298.
- [5] H. Valdez, Lead battery markets and recycling in Mexico and South America, J. Power Sources 67 (1997) 219–223.
- [6] M.A. Kreuzsch, M.J.J.S. Ponte, H.A. Ponte, N.M.S. Kaminari, C.E.B. Marino, V. Mymrin, Technological improvements in automotive battery recycling, Resour. Conserv. Recycl. 52 (2007) 368–380.
- [7] M. Maja, N. Penazzi, M. Baudino, M.V. Ginatta, Recycling of lead/acid batteries: the ginatta process. Proceedings of the international conference on lead/acid batteries, J. Power Sources 31 (1990) 287–294.
- [8] M. Maja, S. Bodoardo, C. Serracane, R. Baudino, Dissolution of pastes in lead acid battery recycling plants, J. Appl. Electrochem. 23 (1993) 819–826.
- [9] R.D. Prengaman, Recovering lead from batteries, J. Met. 3 (1995) 1–33.
- [10] M.V. Ginatta, Method for the electrolytic production of lead, U.S. Patent. 4,451,340 (May 29, 1984).
- [11] M. Olper, Hydrometallurgical process for an overall recovery of the components of exhausted lead acid batteries, U.S. Patent 4,769,116. (September 6, 1988).
- [12] M. Olper, in: J.E. Dutrizac, J.A. Gonzalez, G.L. Bolton, P. Hancock (Eds.), Fluoborate Technology—A New Challenging Way for Primary and Secondary Lead Processing, Zinc and Lead Processing, The Metallurgical Society of CIM, Montreal, 1998, pp. 185–198.
- [13] A.G. Morachevskii, A.I. Demidov, Z.I. Vaisgant, M.S. Kogan, Recovery of lead battery scrap using alkali-glycerol electrolyte, Russ. J. Appl. Chem. 69 (1996) 412–414.
- [14] C. Weiping, T. Yizhunang, B. Kerun, Z. Yue, Basic electrolytic method for recovery of lead from scrap batteries, Trans. Nonferr. Met. Soc. China 6 (1996) 47–51.
- [15] C. Weiping, C. Fancai, P. Yanbing, L. Qizhong, B. Kejun B, Z. Yue, Cathode electrodeposition of lead in Pb^{2+} $-\text{OH}-\text{C}_4\text{H}_4\text{O}_6^{2-}$, Trans. Nonferr. Met. Soc. China 7 (1997) 154–158.
- [16] L.C. Ferracin, E.C.C. Sanhueza, R.A. Davoglio, L.O. Rocha, D.J. Caffeu, A.R. Fontanetti, R.C.R. Filho, S.R. Biaggio, N. Bocchi, Lead recovery from a typical Brazilian sludge of exhausted lead-acid batteries using an electrohydrometallurgical process, Hydrometallurgy 65 (2002) 137–144.
- [17] M. Volpe, D. Oliveri, G. Ferrara, M. Salvaggio, S. Piazza, S. Italiano, C. Sunseri, Metallic lead recovery from lead-acid battery paste by urea acetate dissolution and cementation on iron, Hydrometallurgy 96 (2009) 123–131.
- [18] M.S. Sonmez, R.V. Kumar, Leaching of waste battery paste components. Part 1: lead citrate synthesis from PbO and PbO_2 , Hydrometallurgy 95 (2009) 53–60.
- [19] M.S. Sonmez, R.V. Kumar, Leaching of waste battery paste components. Part 2: leaching and desulphurisation of PbSO_4 by citric acid and sodium citrate solution, Hydrometallurgy 95 (2009) 82–86.
- [20] S. Amrate, D.E. Akretche, C. Innocent, P. Seta, Usage of cation-exchange membranes for simultaneous recovery of lead and EDTA during electrokinetic extraction, Desalination 193 (2005) 405–410.
- [21] F.R. Xiu, F-S. Zhang, Recovery of copper and lead from waste printed circuit boards by supercritical water oxidation combined with electrokinetic process, J. Hazard. Mater. 165 (2005), 1062–1007.
- [22] K.R. Reddy, C. Cameselle (Eds.), Electroremediation Technologies for Polluted Soils, Sediments and Ground Water, John Wiley & Sons Inc., Publication, 2009, p. 6.
- [23] W.M. Latimer, J.H. Hildebrand, Reference Book of Inorganic Chemistry, third ed., The Macmillan Company, New York, 1951, p. 353.
- [24] M.C. Sneed, J.L. Maynard, General Inorganic Chemistry, D. Van Nostard Company, Inc., New York, 1942, p. 975.